Towards Monitoring and Identification of Red Palm Weevil Gender Using Microwave CSRR-Loaded TL Sensors

Mohammed Bait-Suwailam *

Posted Date: 21 June 2023

doi: 10.20944/preprints202306.1533.v1

Keywords: Date palm; CSRR; metamaterials; microwave sensor; red palm weevil

Article

Towards Monitoring and Identification of Red Palm Weevil Gender Using Microwave CSRR-Loaded TL Sensors

Mohammed M. Bait-Suwailam

Sultan Qaboos University; msuwailem@squ.edu.om

Abstract: This paper presents for the first time the design of a microwave sensing setup for the potential monitoring and identification of red palm weevil (RPW) gender type. The microwave sensor consists of a planar two-port transmission line (TL) with a single complementary split-ring resonant (CSRR) inclusion etched from the bottom metallic layer. The CSRR sensor is placed on top of a customized non-conductive container. The microwave sensing setup has been designed, numerically demonstrated, fabricated and tested experimentally. Simulated results correlate quite well with the experimental data. Moreover, the sensitivity of the CSRR sensor when in close proximity to different RPW gender has been evaluated both numerically and experimentally. Based on the measured results from 15 RPW collected samples with different body sizes, different RPW gender types showed unique microwave signatures. Notable shift to the sensor's resonance frequency has been achieved, where on average a resonant frequency shift of 10% for adult RPWs was achieved, while 2.4% frequency change was obtained for larvae (young) RPWs. Hence, the proposed microwave sensing setup can be adopted in field trials to examine and differentiate between various RPW genders at various development stages.

Keywords: date palm; CSRR; metamaterials; microwave sensor; red palm weevil

1. Introduction

Among many harmful insects, red palm weevil (RPW), also known as Asian palm weevil is considered a big threat to date palm trees, especially in the Middle East and North Africa (MENA) region. Such pests have the ability to rapidly grow in short period of time, adopt themselves easily inside the palm trunk in various environmental conditions and can move (travel) from one place to another over several kilometers, due to their abilities to fly. Unfortunately, the rapid spread of RPW pest results in a severe damage to date palm trees, which in turn causes major losses to the economical growth of many developing countries, including many countries within the MENA and Asia regions.

One commonly adopted management control technique for RPW pests is the use of traps. The traps are prepared by filling a container with insect's pheromone mixed with palm odor and water [1,2]. The traps can easily attract RPWs, due to the strong effect of both substances (pheromone mixture with palm odor) in attracting other RPWs. Figure 1a,b depict photos of two collected palm weevil larva and an adult RPW, while Figure 1c shows a captured RPW inset inside a prepared trap in a red container in a local farm.

There have been numerous research studies and efforts in the literature devoted to manage and control the spread of red palm weevil pests, ranging from detecting presence of RPW pests in palm trunks using acoustic signal processing [3], optical distributed sensing [4,5], high power microwave sensing and thermal heating treatment procedures [6–10], among other techniques. The research work in [4] presented a technique for monitoring and detecting RPW by using optical fiber distributed acoustic sensing probes. The sensing system in [4] was able to detect feeding activities of almost 12-days old young RPW, the larvae in an infested palm tree. Massa et al. developed in [6] a high power microwave-based heating system as a potential modality to control and treat palm trees from the invasive RPW. The study in [6] also presented a numerical thermal study in order to estimate

Preprints (www.preprints.org) | NOT PEER-REVIEWED | Posted: 21 June 2023 doi:10.20944/preprints202306.1533.v1

the amount of time required to completely destruct red palm weevil pests. Among the numerical simulation developments related to the RPW control is the work presented in [8], where authors presented an FDTD simulation models to study the effectiveness of microwave energy in isolated RPW irradiation. Based on the numerical simulation results, RPW at larvae stage was found to absorb sufficient electromagnetic energy that leads to complete destroy of RPWs. Another numerical study of microwave heating of RPW was also presented in [9], in which authors developed an array of vivaldi antenna. In the study, the main focus was on thermal treatment of the infested palm trees through the use of high power microwaves. Based on the findings from [6,9], it was concluded that high-power microwaves are effective mechanism for reliable destruction of palm weevils.

Figure 1. Photos taken from a local date palm farm, showing collected palm insects from infested palm tree (a) larva (b) adult RPW, and (c) an adult RPW captured inside of a prepared field trap.

To the best of our knowledge, there are no major developments or comprehensive studies for the identification of RPW gender type, especially with the help of low-power microwave sensors. The contributions in this research study are summarized below:

1. develop microwave CSRR-loaded transmission line (TL) sensors for potential identification and detection of RPW gender type through the recording of the transmission strength of the sensor.
2. present 3D numerical models that mimic the nature of microwave CSRR sensors in the detection of various RPW genders.
3. present an experimental setup of the microwave identification setup for RPW gender detection. Due to the limited access to collection of RPWs, only samples were considered in the experimental study.
4. earlier studies have focused on microwave heating treatment of date palm trunks infested with RPW pests. However, this research work explores deeply the effectiveness of the microwave CSRR probes when interacting with RPW pests towards identification of RPW different gender types.
5. this study also assesses the performance of the microwave CSRR sensor over a population of 17 RPW samples that were collected from a local infected date palm farm: 5 samples for adult male RPW, another 5 for adult female RPWs and 7 samples for larvae insects.
6. this study focuses mainly on isolated RPW samples of various gender types, which is important to quantify the strength and effectiveness of the developed microwave sensor. Future studies will aim into investigating the applicability of machine learning on estimating RPW gender type in a more populated area with different RPW gender and species at different stages. Further, this research study contributed to the field of RPW pests control through the deployment of low-power microwaves to investigate potential identification of RPW gender instead of the high-power microwave treatments, which had been reported in earlier studies. Thus, avoiding the needs of using harmful radiation that farmers could be exposed to during their daily work.

Due to the vast variations of electric properties of the RPW at its different life development stages, we believe that microwave CSRR transmission line based sensors are attractive to deploy. This is due to their low profile, ease of fabrication and narrowband sensing capability. The microwave sensor

Preprints (www.preprints.org) | NOT PEER-REVIEWED | Posted: 21 June 2023 doi:10.20944/preprints202306.1533.v1

is placed on top of the sensed RPW pest with a small controllable stand-off distance. In this study, numerical full-wave simulations are presented and validated with experimental results, where all materials' properties of the setup including the RPW types are included in the simulation models.

2. Numerical simulations of RPW gender identification

2.1. Numerical modeling of the CSRR Sensor

In the past twenty years, the integration of small-resonant metamaterial particles, in the form of split-ring resonators (SRRs) [11] or complementary split-ring resonators (CSRRs) [12], in planar microwave transmission lines have led to numerous developments and enhancement to sensory elements and devices in many applications, including but not limited to radio frequency microwave circuits, materials characterization and classification [14–17]. Complementary SRR can be regarded as a quasi-static resonator, when its dimension is electrically small as compared with the operating wavelength of the excitation electromagnetic field. In such a case, the microwave CSRR resonance frequency is attributed to the equivalent *LC*-resonant tank circuit upon an excitation of an external normal electric field component to the resonator's surface area, i.e., z-direction in Figure 2, where the current flow circulating around the CSRR metallic rings contributes to the inductance L, while the cuts (slots) in the two rings results in a developed distributed capacitance effect C. The resonance frequency of the CSRR can then be estimated using

$$f_{res} = \frac{1}{\sqrt{L_{dist} * C_{dist}}} \tag{1}$$

where f_{res} is the resonant frequency of the CSRR sensor, L_{dist} and C_{dist} are the total distributed inductance and capacitance of the CSRR sensor, respectively. The dimensions of the designed microwave CSRR unit inclusion (see Figure 2 (b)) were initially estimated using the relations provided in [18–20] based on the resonance frequency of the CSRR from the retrieved effective electric permittivity response. A slight shift in the resonance frequency would be expect, since the CSRR resonator is coupled to the transmission line. As such, optimized dimensions are then obtained through trained simulation tasks, which requires the consideration of the capacitive coupling between the rings for a more accurate estimation of the sensor's resonance frequency.

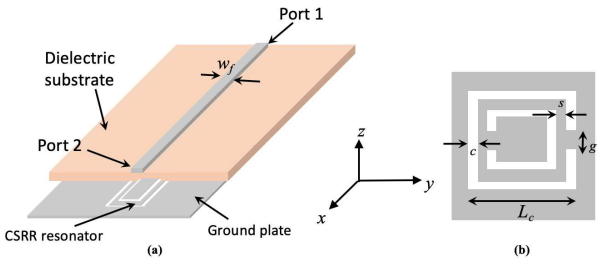

Figure 2. (a) Schematic of the CSRR probe, (b) the complementary split-ring resonator with its design parameters. The grey area represents metallization.

In this work, we deploy microwave CSRR transmission line based sensor as a promising near-field probe for identifying RPWs gender, taking into account the advantages of such sensors in terms of high sensitivity and narrowband operational band. Figure 2 (a) shows the microstrip transmission line CSRR sensor, where a single CSRR inclusion is etched out from the metallic solid ground layer, with a transmission line width of w_f = 3.05 mm corresponding to a 50-Ω port impedance. Figure 2 (b) shows a schematic for a complementary split-ring resonator unit cell. The optimized dimensions of the CSRR sensor are: L_c = 9 mm, s = 1.575 mm c = 0.45 mm and g = 0.5 mm, where its resonance frequency is 2.45 GHz, within the ISM frequency band. For convenience, an FR-4 square laminate of dimension 6 x 6 mm^2 (with a dielectric constant of 4.4 and a loss tangent of 0.02) and thickness of 1.6 mm was chosen

Preprints (www.preprints.org) | NOT PEER-REVIEWED | Posted: 21 June 2023 doi:10.20944/preprints202306.1533.v1

as the host medium of the microwave CSRR sensor. Figure 3 shows the scattering parameters response both reflection and transmission coefficients of the modeled microwave CSRR-TL sensor. The sensor resonates quite well at 2.45 GHz-ISM band, as can be seen from the S_{21} response, with a dip of -20 dB.

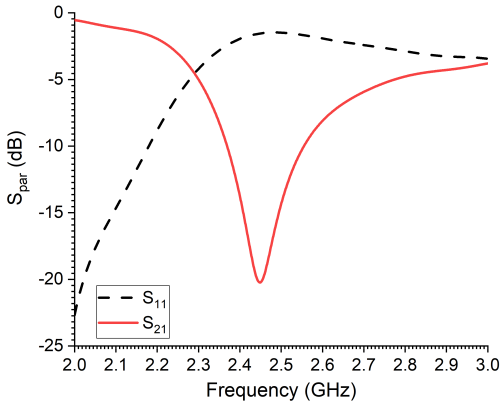

Figure 3. The simulated reflection and transmission coefficients, S_{11} and S_{21} respectively, of the developed transmission line based CSRR sensor.

2.2. Numerical setup of the RPW gender detection system

Figure 4 depicts the numerical setup showing a 2-mm thick rectangular container, (mimicking a small cardboard, with a dielectric constant of 2.7). For convenience, the dimension of the container is used as: L x W x H = 60 x 60 x 10 mm^3. An adult RPW is modeled here as an elliptical cylinder (D_1 x D_2 x 1.5 mm) and is placed at the center of the container from its base. In order to have a more realistic scenario for the modeled adult RPW, a thin nose was attached to the body of the pest with a length of L_{ext} = 10 mm.

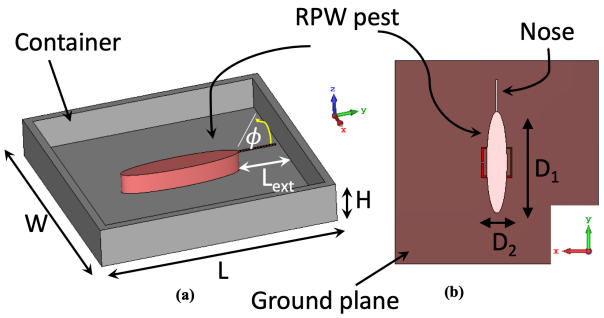

Figure 4. The developed numerical setup to study variations on detecting RPW pest gender type: (a) perspective view of the container with the modeled adult RPW, (b) bottom view of the microwave CSRR sensor with the RPW pest.

Next, we present a numerical parametric study to investigate the strength of the developed CSRR sensor in predicting changes to the RPW size, where D_2 is kept constant at 6 mm, while D_1 is arbitrarily varied. The incurred percentage shift in the sensor's resonance frequency can be estimated using

$$F_{res}Change = \frac{(F_{ref} - F_{RPW})}{F_{ref}} X100\% \quad (2)$$

where $F_{res}Change$ is the percentage shift in the resonant frequency of the probe in % when the sensor is in close contact to the RPW insect, F_{ref} is the resonance frequency of the probe alone (unloaded), while F_{RPW} is the resonance frequency of the probe when in contact with the RPW. Figure 5 depicts the percentage shift of the sensor's resonance frequency when in close proximity to the modeled adult

Preprints (www.preprints.org) | NOT PEER-REVIEWED | Posted: 21 June 2023 doi:10.20944/preprints202306.1533.v1

RPW when the size of the pest D_1 is increased from 6 mm to 30 mm. Clearly, there is an increase in the sensitivity strength of the probe as the aperture size of the RPW is increased, which is quantified through recording the sudden horizontal resonant frequency shift of the transmission coefficient minimum (dip).

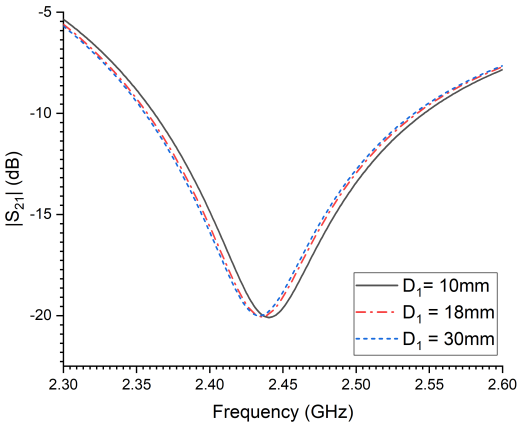

Figure 5. The percentage shift in the sensor's resonance as a function of the adult RPW pest length, D_1.

It is very important to consider all dielectric losses associated with the modeled RPW at their development stages, namely: larva, pupal chamber and adult. The dielectric constant and loss factor of three RPW genders were estimated from earlier measured data in [21] at 2.45 GHz, which are summarized and presented in Table 1. Figure 6 presents the numerical results of detecting movements of a small RPW larva, where a horizontal rotational movement, i.e., in terms of angle ϕ in Figure 4(a), is varied within the xy-plane. It can be seen from Figure 6 that the CSRR resonance frequency tends to shift to lower frequencies as the rotational angle ϕ is increased from 0° to 90°, where angle of 90° corresponds to an orientation that is perpendicular to transmission line segment of the sensor. Moreover, the tendency of the sensor's detection is quite noticeable and appreciable. Hence, the findings from this numerical study is valuable in tracking small movement activities of the RPW, especially during feeding stages.

Table 1. The dielectric properties of various RPW gender at the 2.45 GHz-band estimated from the measured dataset available in [21].

RPW gender type	Dielectric constant	Loss tangent
Larva	38	12.5
Pupal chamber	39.5	8.5
Adult RPW	7.5	0.125

Figure 7 depicts a numerical study showing the sensing capability of the CSRR probe in identifying variations to RPW at its various development stages. A 40-MHz shift in the sensor's resonance frequency is achieved, which is its ability to differentiate between an adult RPW and either larva or pupal chamber. This is attributed to the less water content and moisture of the adult RPW as compared to the larva and chamber. Moreover, from the simulated results, there was no noticeable change in the sensor's resonance frequency for the cases of larva and pupal chamber, due to the similarities in body shape of both young insects and similarity in their electric properties.

Preprints (www.preprints.org) | NOT PEER-REVIEWED | Posted: 21 June 2023 doi:10.20944/preprints202306.1533.v1

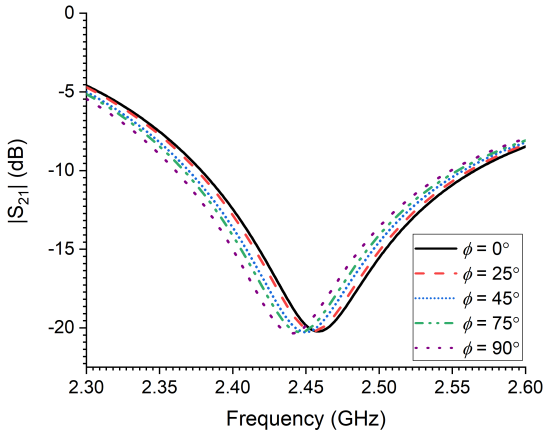

Figure 6. The simulated transmission coefficient of the sensor as a function of RPW larva orientation (rotational movement, ϕ).

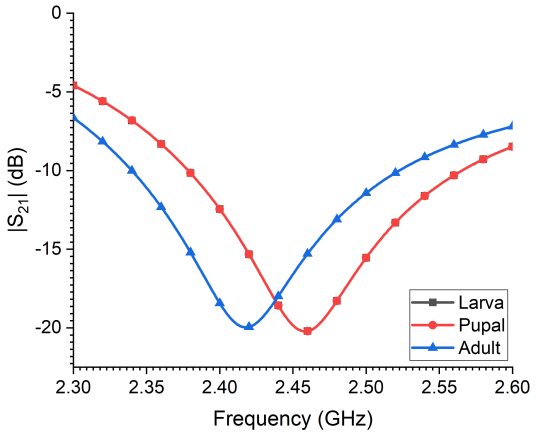

Figure 7. The simulated transmission coefficient of the sensor for modeled RPW at three different development stages: larva, pupal chamber and adult.

Figure 8 presents the simulation results from a numerical parametric study showing the effect of the stand-off distance, i.e., vertical distance, between the top (body) surface of the RPW insect and the CSRR ground layer (bottom layer of sensor). In this parametric study, an adult and a pupal chamber insects are considered. As can be seen, the shift in CSRR resonance frequency is quite significant for the adult case as compared against the pupal case when the sensor is touching both the adult and the pupal insects, $stand-offdistance = 0.0$. The sudden resonance shift in the case of adult RPW is due to the minimal inherent dielectric losses of adult RPW as compared against a young insect. Furthermore, both cases reach minimal shift in resonance as the vertical stand-off distance is increased, which was kept at 3 mm for convenience. As such, a stand-off distance between 0.5 mm - 1.5 mm could be used in order to observe higher sensitivity, especially for the case of young RPW insects, since they tend to absorb significant amount of microwave energy and hence reduce sensitivity strength.

Preprints (www.preprints.org) | NOT PEER-REVIEWED | Posted: 21 June 2023 doi:10.20944/preprints202306.1533.v1

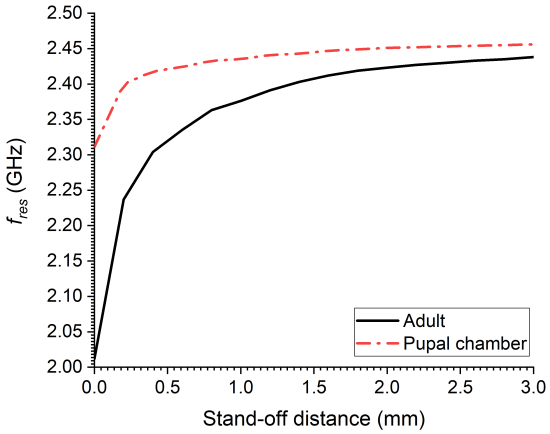

Figure 8. The simulated transmission coefficient of the sensor for modeled RPW at three different development stages: larva, pupal chamber and adult.

3. Experimental Results

Figure 9 depicts the experimental setup of the RPW gender identification using the developed CSRR sensor. In Figure 9(a), an adult RPW (collected from an infested palm tree) was attached to the base of a thin paper container using a thin non-conducting tape. The microwave CSRR sensor was fabricated in-house using CNC milling machine with two edge-SMA connectors attached to the 50-Ω transmission line for measurement. After calibration, the fabricated sensor was then placed on top of the container and the two ports were connected to the vector network analyzer in order to measure its transmission coefficient.

(a) (b)

Figure 9. Two photos demonstrating the experimental setup, (a) male RPW kept in place inside a paper-based container, (b) the microwave CSRR sensor on top of the male RPW pest.

In order to ensure reliability of the microwave CSRR sensor's sensing capability, a population of 17 RPW pest samples were collected from a local date palm farm, where 10 samples for adult RPWs were collected (5 for each male and female RPWs) and 7 samples from larva pests were collected in maintained air flow containers, as can be seen from Figure 10. Note that it is possible to differentiate between male and female adult RPW while collecting the samples in the field by observing little brownish hair in the nose of the male RPW unlike the female RPW which do not have such hair present in its snout. A magnifier was used for that purpose. Due to the rapid movement and activity of the RPW pests under test, it was necessary to use a light flexible transparent tape in order to gently maintain the RPW under test and keep it witin a referenced location inside the sensing container as illustrated in Figure 9. Table 2 presents the summary of the CSRR sensor's percentage frequency

Preprints (www.preprints.org) | NOT PEER-REVIEWED | Posted: 21 June 2023 doi:10.20944/preprints202306.1533.v1

shift using Equation (2) from the experimental results conducted on 15 RPW samples (5 samples for each male, female and larvae). The averaged percentage change was around 10% for adult RPWs (male/female), while it was around 2.4% for young larvae insects.

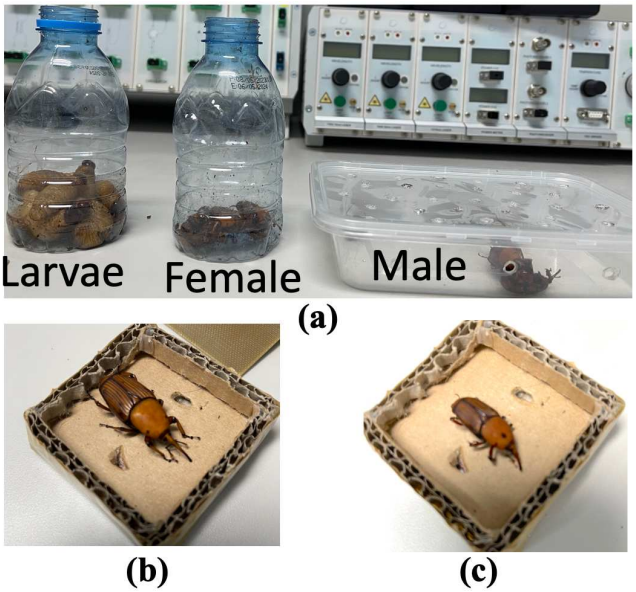

Figure 10. (a) The collected RPW samples considered in this study (male, female and larvae RPWs), (b) a big size adult male RPW, and (c) a small size adult male RPW.

Table 2. Estimated frequency shift of the microwave CSRR sensor when in near-field proximity to various RPW pests in reference to unloaded CSRR sensor.

Sample no.	Male RPW	Female RPW	Larvae
1	3.79	7.03	0.65
2	4.20	7.43	1.33
3	8.24	7.43	1.37
4	11.48	14.30	3.80
5	13.08	19.15	4.61
AVG.	9.46	9.78	2.35

For calibration purposes, the performance of the sensor was first recorded alone, after which, the sensor was assessed when exposed to some selected RPW samples in order to sense both back and front body surface. Table 3 presents the resonant frequency of the CSRR sensor. As can be seen from Table 3, no major changes to the sensor's resonance frequency from both front (wings side) and back (belly side) surfaces of RPW samples, except for less than 60 MHz frequency between front and back sides of the three tested samples.

Table 3. The CSRR sensor's resonance frequency when exposed to male, female and larva RPW from front (wings side) and back (belly side).

surface type	Male RPW	Female RPW	Larvae
Front	2.32	2.42	2.46
Back	2.26	2.41	2.44

Figure 11 depicts the measured the sensor's resonance frequency per sample under test, where sample numbers are given in order as per the insect's size and body shape. In other words, sample 1

Preprints (www.preprints.org) | NOT PEER-REVIEWED | Posted: 21 June 2023 doi:10.20944/preprints202306.1533.v1

corresponds to a RPW insect with the smallest possible size within the samples' collection (whether male, female or larva),while sample 5 corresponds to the biggest RPW under test from the samples collection. For comparison purposes, 5 samples from larva were also selected. As can be seen from Figure 11, the sensor's resonance frequency shows minimal changes to the case of sensing the whole 5 samples of larva, which is expected since larvae do have a cylindrical body with minimal changes to their body size, as compared against the adult RPW (male or female). Further, there was a big shift in the sensor's resonance frequency for the case of female RPW sample 5, which corresponded to a quite large size insect.

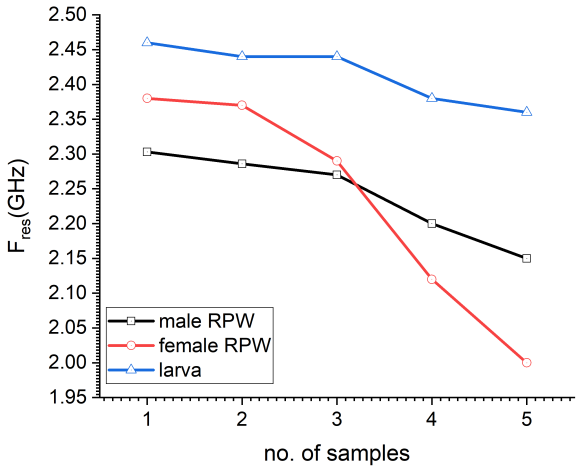

Figure 11. The measured resonance frequency of the sensor for 15 samples of RPW gender, with 5 samples for each male, female and larva pests.

Figure 12 presents the measured resonance frequency of the CSRR sensor when exposed to a single RPW sample under under 4 potential rotational mechanisms (see Figure 4): 0^o, 90^o, 180^o, 270^o and 360^o, which reflects the movement of the RPW insects. From the presented measured data, we could see minimal changes to the detected resonance of the CSRR sensor that was less than 70 MHz. This is justified due to the variation of electromagnetic field distribution when exposed to the RPW sample under the rotational movement cases.

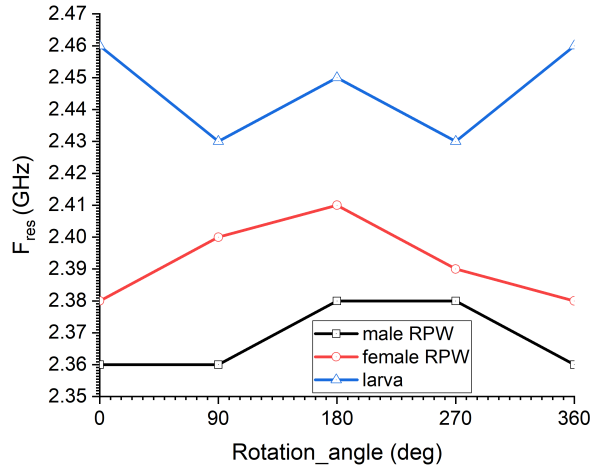

Figure 12. The measured resonance frequency of the sensor as a function of the rotational angle, ϕ, where angle ϕ is illustrated in Figure 4.

Preprints (www.preprints.org) | NOT PEER-REVIEWED | Posted: 21 June 2023 doi:10.20944/preprints202306.1533.v1

Figure 13 depicts the measured transmission coefficient of the microwave CSRR sensor as a function of frequency for 5 samples of adult male RPWs. We could see that sensor's resonance for samples 4 and 5 have not changed, since the two last samples of male RPWs are comparable in size. Moreover, similar trend in the sensor's detection strength was observed for the 5 female RPW samples under test, in which an increased frequency shift to the resonant frequency towards lower frequency regime can be seen as the female RPW size gets larger.

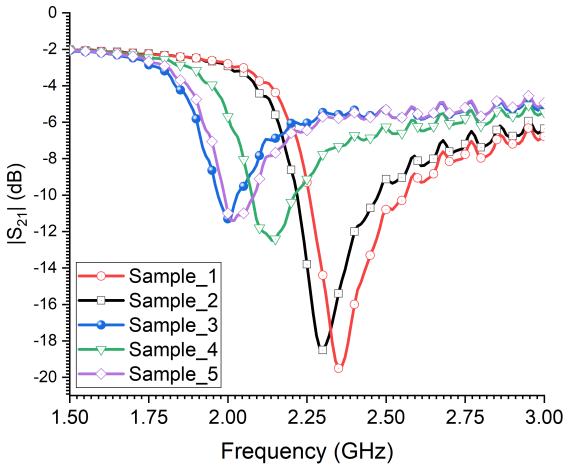

Figure 13. The measured transmission coefficient of the sensor when exposed to 5 adult male RPW insects with different body sizes.

The assessment of detecting adult female RPWs gender using the CSRR sensor can be seen from Figure 14. In this case, the sensor has not recorded much changes in its resonance frequency for the 1st three samples, when compared with the last two samples, i.e., samples 4 and 5. That is because the first three samples were quite comparable in body shape and size.

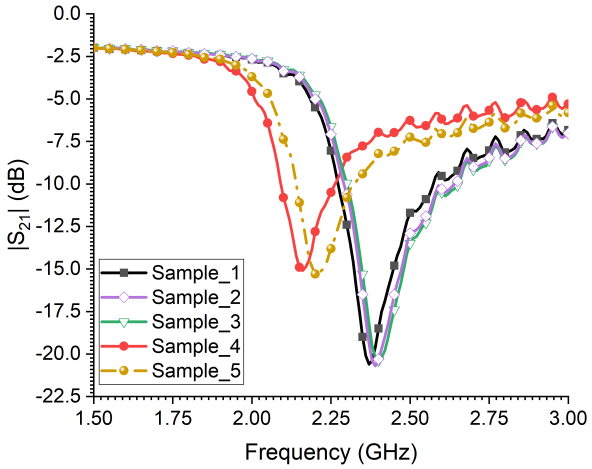

Figure 14. The measured transmission coefficient of the sensor when exposed to 5 adult female RPW insects with different body sizes.

Lastly, the measured transmission coefficient of the CSRR sensor when exposed to 7 samples of larvae is presented in Figure 15. Interestingly, not much change to the sensor's resonance was observed for the larvae samples. This is justified since all samples are of similar body size and qualitatively an indication of similar body losses. Moreover, there is a quite higher frequency shift of the sensor towards lower frequency regime for sample 7, which corresponds to a large larva size.

Preprints (www.preprints.org) | NOT PEER-REVIEWED | Posted: 21 June 2023 doi:10.20944/preprints202306.1533.v1

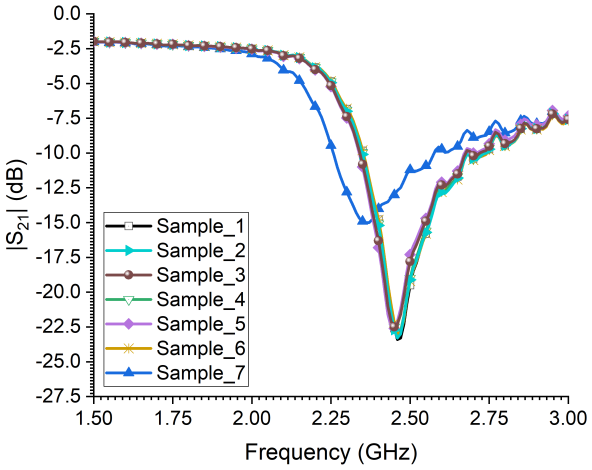

Figure 15. The measured transmission coefficient of the sensor when exposed to 7 larvae RPW insects with different body sizes.

Although the developed microwave CSRR sensor was able to differentiate existence of single and dual RPW within the aperture area of the sensor, we believe that the use of multiple (cascaded) CSRR rings within the sensor could enhance further the possibility of the sensor in differentiating more than two RPW pests when placed in the same aperture area of the sensor. Another issue that could limit the high prediction of the current developed CSRR sensor is the prediction of RPW gender due to random mobility of RPW pests could be enhanced with the deployment of artificial intelligence based models.

4. Conclusions

In this paper, a low-cost microwave CSRR sensor has been developed and tested for the identification and monitoring of red palm weevil gender for the first time. The sensor is composed of a two-port transmission line loaded with CSRR inclusion that is etched out from a bottom metallic layer.A full-wave numerical simulations were carried out and demonstrated with experimental results for validation purposes. The microwave sensor is fabricated using standard printed circuit board technology, which makes its deployment as a RPW inspection tool very effective and attractive.
Based on the the simulated results and measured data, the CSRR probe was able to detect variations on RPW gender types, where the the average percentage frequency shift of the sensor for adult RPW samples resulted in almost 10%, while it was 2.4% when sensing young larvae samples. From the findings of this numerical and experimental study, microwave CSRR-based sensors are found promising candidates for the detection and classification of RPW genders, due to the reduced cost of fabrication as well as simplicity in the sensing system setup.

Acknowledgments: The author would like to thank Oman Telecommunications Company for providing the financial needs to accomplish this research project.

References

1. A. Al-Saoud, M. Al-Deeb, and A. Murchie, “Effect of color on the trapping effectiveness of red palm weevil pheromone traps," *Journal of Entomology*, vol. 7, pp. 54-59, 2010.
2. M. Soomro, J. Mari, I. Nizamani, and A. Gilal, “Performance of ferrolure+pheromone in the red palm weevil, Rhynchophorus ferrugineus (Coleoptera: Dryophthoridae) management in date palm growing areas of Sindh, Pakistan," *Journal of Saudi Society of Agricultural Sciences*, vol. 21, pp. 114-124, 2022.
3. V. Nangai, and B. Martin, “ Interpreting the acoustic characteristics of RPW towards its detection - a review," *IOP Conference Series: Materials Science and Engineering*, vol. 225,p. 012178, 2017.

4. I. Ashry, et al., "Early detection of red palm weevil using distributed optical sensor," *Scientific Reports*, vol. 10, p. 3155, 2020.
5. B. Wang, et al., "Towards detecting red palm weevil using machine learning and fiber optic distributed acoustic sensing," *Sensors*, vol. 21, p. 1592, 2021.
6. R. Massa, et al., "Experimental and numerical evaluations on palm microwave heating for red palm weevil pest control," *Scientific Reports*, vol. 7, p. 45299, 2017.
7. M. Bini, et al., "A protable microwave system for woodworm disinfestation of artistic painted boards," *Journal of Microwave Power and Electrom. Energy*, vol. 32, no. 3, pp. 180-187, 1997.
8. I. Ali, A. Al-Jabr, and A. Memari, "FDTD simulation and experimental investigation of controlled microwave irradiation of red palm weevils," *In the 2010 IEEE Middle East Conference on Antennas and Propagation*, pp. 1-8, 2010.
9. H. Rmili, K. Alkhalifeh, M. Zarouan, W. Zouch, and M. T. Islam, " Numerical analysis of the microwave treatment of palm trees infested with the red palm weevil pest by using a circular array of vivaldi antennas," *IEEE Access*, vol. 8, pp. 152342-152350, 2020.
10. M.M. Bait-Suwailam, " Numerical assessment of red palm weevil detection mechanism in palm trees using CSRR microwave sensors," *Progress In Electromagnetics Research Letters*, vol. 100, pp. 63-71, 2021.
11. J.B. Pendry, A. J. Holden, D. J. Robbins, and W. J. Stewart, "Magnetism from conductors and enhanced nonlinear phenomena," *IEEE Transactions on Microwave Theory and Techniques*, vol. 47, no. 11, pp. 2075–2084, 1999.
12. F. Falcone, et al., "Analysis of stripline configurations loaded with complementary split ring resonators," *Microwave and Optical Technology Letters*, vol. 55, pp. 1250-1254, 2013.
13. F. Falcone, T. Lopetegi, J. D. Baena, et al., "Effective negative-stopband microstrip lines based on complementary split ring resonators," *IEEE Microwave and Wireless Components Letters*, vol. 14, no. 6, pp. 280–282, 2004.
14. M. S. Boybay and O. M. Ramahi, "Material characterization using complementary split-ring resonators," *IEEE Trans. Instrum. Meas.*, vol. 61, no. 11, pp. 3039– 3046, 2012.
15. M. H. Zarifi and M. Daneshmand, "Non-contact liquid sensing using high resolution microwave microstrip resonator," 2015 IEEE MTT-S International Microwave Symposium, Phoenix, AZ, USA, pp. 1-4, 2015.
16. A. Lavado, et al.," Low-cost electromagnetic split-ring resonator sensor system for the petroleum industry," *Sensors*, vol. 22, p. 3345, 2022.
17. S. Eom, and S. Lim, "Stretchable complementary split ring resonator (CSRR)-based radio frequency (RF) sensor for strain direction and level detection," *Sensors*, vol. 16, p. 1667, 2016.
18. S. Maslovski, et. al, "Artificial magnetic materials based on the new magnetic particle: Metasolenoid," *Progress In Electromagnetic Research*, vol. 54, pp. 61-81, 2005.
19. J. Baena, et. al, "Equivalent-circuit models for split ring resonators and complementary split-ring resonators coupled to planar transmission lines," *IEEE Trans. on Microwave Theory and Techniques*, vol. 53, no. 4, pp. 1451-1461, 2005.
20. M.M. Bait-Suwailam, L. Yousefi, B. Alavikia, and O. Ramahi, "Analytical models for predicting the effective permittivity of complementary metamaterial structures," *Microwave and Optical Technology Letters*, vol. 55, no. 7, pp. 1565-1569, 2013.
21. R. Massa, et al., "Wide band permittivity measurements of palm (Phoenix canariensis) and Rhynchophorus ferrugineus (coleoptera curculionidae) for RF pest control," *Journal of Microwave Power and Electromagnetic Energy*, vol. 48, pp. 158-169, 2014.